ARTICLE

# Construction of the Apparatus for Two Dimensional Electronic Spectroscopy and Characterization of the Instrument†

Shuai Yue, Zhuan Wang, Xiao-chuan He, Gang-bei Zhu, Yu-xiang Weng*

*Laboratory of Soft Matter Physics, Institute of Physics, Chinese Academy of Sciences, Beijing 100190, China*

(Dated: Received on June 25, 2015; Accepted on July 12, 2015)

This work describes the construction of a phase-stable two dimensional electronic spectrometer operating in a photon echo mode with optical heterodyne detection, where the diffractive optics were used to realize the passive phase stabilization. In addition, a high speed and sensitive EMCCD was configured for shot-to-shot measurement which effectively improved signal-to-noise ratio. Consequently, the phase stability between a pulse pair split by the diffractive optics was determined in terms of standard deviation to be $\lambda/200$ during an observation period of 30 min, while the phase stability of the photon echo signal measured with IR140 is $\lambda/90$ in 19 min. In addition, a method of phase-shift in the pump pulse is also presented, which can effectively remove the interference from scattering light in collection of pump-probe transient absorption spectrum. The phase-shift method can improve the accuracy of phase adjustment in 2D electronic spectrum of scattering samples.

**Key words:** Two-dimensional electronic spectroscopy, Phase stability, Phase adjustment

## I. INTRODUCTION

Multi-dimensional optical Fourier transform spectroscopy (FTS) originates conceptually from the development of nuclear magnetic resonance (NMR) [1], where the basic physical principles underlying multi-dimensional NMR have been transferred to the spectral region of optical wavelengths, and the probed electronic transitions reveal the electron distributions in the excited state that correlate to the associated molecular structure and bath dynamics. For condensed phase systems, the time scales involved in relaxation and dephasing phenomena of excited electronic states are in the femtosecond regime [2]. However, due to the problem arising from the Fourier transformation limit imposed by the pulse, *i.e.*, a short pulse has a broad spectrum [3], both pump and probe frequency resolved ultrafast relaxation process can hardly been realized by means of conventional spectrometer. As to the spectral resolution in the probe spectrum, several groups have already spectrally resolved short probe pulses after they traversed a pumped sample. This allows coherent molecular radiation in the probe direction, which may continue after the probe exists in the sample, which can provide a spectral resolution much better than that limited by the probe pulse [4]. However, the pump pulse still imposes an externally fixed Fourier transformation limited trade-off between time resolution and spectral resolution. 2D Fourier transformation (2D-FT) spectra could provide the pump-probe correlation for molecules in both frequency dimensions [3]. Performing the 2D-FT of the experimentally measured nonlinear optical response function, the 2D frequency-resolved optical spectrum can be obtained in principle. Whereas in practice, one dimensional Fourier transformation giving the probe frequency is always realized by a conventional spectrometer, leaving the pump frequency to be resolved from the time space. The obvious advantage of 2D-FT spectrum over traditional one dimensional spectroscopy is that it can disentangle congested spectrum by spreading the spectrum out over two dimensions, and coupling between resonances can be identified by the presence of cross-peaks in the 2D spectrum. Fourier transform spectroscopy is an ideal tool for unraveling coupling among resonances and dynamics in complex systems [5]. 2D spectroscopy has been developed experimentally by Jonas's group in the near IR region [6, 7]. In the visible region, 2D spectroscopy was implemented by the groups of Fleming *et al.* [8], Miller *et al.* [9], Scholes *et al.* [10], Ogilvie *et al.* [11]. Two-dimensional electronic spectroscopy (2DES) has become a powerful tool suitable for studying of electronic couplings in multichromophore molecular aggregates [12], coupled quantum dots [13], and other systems.

2DES probes photo-initiated electronic dynamics on ultrafast timescales [14]. One implement of the 2DES is photon echo experiment, *i.e.*, three ultrashort pulses are arranged in a unique temporal sequence to excite

†Dedicated to Professor Qing-shi Zhu on the occasion of his 70th birthday.

*Author to whom correspondence should be addressed. E-mail: yxweng@aphy.iphy.ac.cn

 

the sample, creating a 3rd order polarization $P^{(3)}$, and the fourth homologous laser pulse serving as a local oscillator to detect the emitted signal by means of optical heterodyne detection.

The two pump pulses 1 and 2, are separated in time by the evolution period $\tau$, followed by the probe pulse 3 after a population waiting time $T$. The 2D spectrum at a particular $T$ involves frequency dimensions $\omega_t$ and $\omega_\tau$, corresponding to the detection period $t$ and evolution period (coherence time) $\tau$ respectively. The detected signal $S(\tau, T, \omega_t)$ by the spectrometer is related to the 3rd polarization $P^{(3)}(\tau, T, t)$ via one dimensional Fourier transformation on the detection period $t$ at the phase-matched condition $K_s = K_1 - K_2 + K_3$

$$\begin{aligned}\tilde{S}(\tau, T, \omega_t) &= i.sig(\omega_t) \int_{-\infty}^{\infty} P^{(3)}(\tau, T, t) \exp(i\omega_t t) \mathrm{d}t \\ &= i.sig(\omega_t) \tilde{P}^{(3)}(\tau, T, \omega_t) \end{aligned} \quad (1)$$

where the 3rd-order polarization is related to the measured signal field by

$$\tilde{P}^{(3)}(\tau, T, \omega_t) \propto \frac{\tilde{E}(\tau, T, \omega_t)}{\omega_t} \quad (2)$$

Qualitatively, $\mathrm{Re}\{\tilde{S}(\tau, T, \omega_t)\}$ contains information regarding the effect of initial pump with a coherence time $\tau$ on the probed absorption at $\omega_t$ after a population time $T$ [15, 16].

In general, one of the most challenging requirements of coherent 2DES in a noncollinear photon-echo geometry is the relative phase stability of the laser pulses that generate and measure the nonlinear signal. Small drifts or vibrations of beam splitters and mirrors would lead to drift of the signal phase, therefore, after Fourier transformation this would give rise to distortions in the 2D spectra. The situation is even more critical in the 2DES than that in 2DIR because of the shorter wavelength, which typically does not allow conventional splitting, delaying, and recombining of laser beams [17].

For limited bandwidth, passive phase stabilization strategy by using diffractive optics (DO), *i.e.*, gratings [2, 16, 18, 19] as the beam splitters have been implemented in the 2DES. In these schemes, small vibrations of the diffractive beam splitter and the imaging confocal mirrors do not change the phase between the two diffracted pulses significantly because both beam paths change by the same amount [16]. Another advantage of using the DO is that the spilt beams can be perfectly overlapped with their pulse fronts within the sample via a 4f imaging setup [20].

In this work, we present the construction of a DO-based 2DES implementation, together with characterization of its main specifications. 2D spectra of IR144 dye solution and a photosynthetic subunit B820 isolated from the photosynthetic bacteria were collected and processed, the results are comparable to those previous studies [21]. Furthermore, we report a method for acquisition of pump-probe transient absorption spectrum when the sample having a significant light scattering effect by a phase shift technique, which is used for phase adjustment in 2DES.

## II. EXPERIMENTS

### A. Sample preparation

Laser dyes IR144 and IR140 were used as received from Exciton. The subunit B820 of light harvesting antenna complex LH1 in the presence of 1% ($w/V$) $n$-octyl $\beta$-D-glucopyranoside ($\beta$OG, Aldrich) was isolated from the chromatophores of *Rhodospirillumrubrum* G9 bacteria as described by Miller *et al.* [22]. All of the solvents were of analytical grade. The samples were recycled by peristaltic pump with a rate about 0.1 m/s during the measurement.

### B. Apparatus for 2DES

Our construction of the 2DES follows the traditional version of the diffractive optics [2] and the experimental apparatus is shown in Fig.1. A commercial Ti:sapphire laser (Spitfire Ace, Spectra Physics) with a pulse width of 35 fs, working at a repetition rate of 500 Hz, and a central output wavelength at 790 nm with approximately 30 nm spectral width is used as the light source for the implementation of 2DES. At first, the laser beam is split into two beams with the same amount of chirp by a pair of 0.5 mm-thick beam splitters. One of the beams is delayed by an electrically controlled translation stage (ST-T, M-521.DD, Physik Instrumente) to realize the population time $T$ with a resolution of 0.67 fs. Then these two beams are focused onto a transmission grating (diffractive optics, 80 grove/mm) through a spherical mirror SM1 ($f$=300 mm). The first order ($m$=+1 and $m$=−1) diffractions of these two beams are picked up as the excitation pulses 1, 2, 3 and pulse 4 (local oscillator, LO) for heterodyne detection. After passing through the grating, all of these four beams are collimated with a spherical mirror SM2 ($f$=250 mm). Two fused silica wedge pairs (thickness 1.5 mm, wedge angle 1°) are inserted into the beam 1 and 2 separately to provide the coherence time $\tau$. One of optical wedge in each pair is set on a precisely controlled translation stage (ST1 and ST2, M-122.2DD, Physik Instrumente) respectively with a step increment of 0.2 μm. The thickness change caused by insertion of optical wedge can provide a time increment of 5.3 as. A 2.5 mm fused silica plate is inserted into beam 3 to balance the dispersion introduced by the wedges in beam 1 and 2. The intensity of LO is attenuated to about three orders in magnitude by a neutral density (ND) filter. And the thickness of the ND filter is slightly thinner than the balance silica plate to make the LO pulse precede the other pulses by about

DOI:10.1063/1674-0068/28/cjcp1506136 

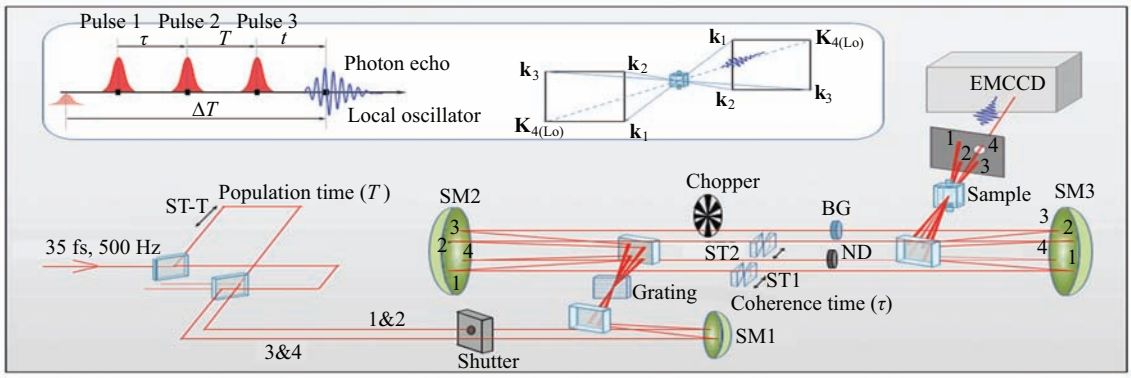


FIG. 1 Experiment setup, a beam of femtosecond laser is split by a pair of 0.5 mm splitter (BS1, BS2). The split beams being focused by a spherical mirror SM1($f$=300 mm) onto a grating. The first orders provide the first three excitation pulses as well as the local oscillator. All of the beams being collimated with a spherical mirror SM2($f$=250 mm) and focused by SM3 ($f$=300 mm) into the sample. Time delays provided by step stages (ST-T, ST1, ST2), an automated beam shutter and an optical chopper being used to remove the scattering signal and the local oscillator from the heterodyne spectrum.

750 fs. Finally, all of the four beams are focused into a fused silica sample cell with an optical length of 200 μm by another spherical mirror SM3 ($f$=300 mm). The thickness for both the front and back wall of the sample cell are 0.9 mm. By moving the delay stage ST2 to make pulse 2 preceding to pulse 1, the rephasing signals will be generated in the same direction of the LO pulse. While the nonrephasing signals can be generated simply by reversing the timing sequence of pulse 1 and 2 through moving the delay stage ST1. Afterward, the heterodyne signals created between the photon echo pulse and the LO pulse are collected by an EMCCD coupled spectrometer (SP2358, Princeton Instrument). To reduce the noise and enhance the speed of data acquisition, a shot-to-shot measurement strategy has been implemented, *i.e.*, the third laser beam is chopped to a frequency to half of the repetition rate of the laser source, the intensity of the LO and the heterodyne signals are recorded by the EMCCD at every other pulse. Furthermore, the CCD gating time was set as 100 μs, so that the random noise would be reduced in proportional to $N^{-1/2}$ where $N$ is the number of a single-shot signals recorded for averaging. In the current case, every one hundred acquired single-shot signals for the LO and heterodyne signals are averaged respectively, these averaged results are stored in PC as the raw data. As a result, the shot-to-shot data acquisition procedure achieves a higher data acquisition speed and higher signal-to-noise ratio in contrast to the commonly used CCD multi-pulse integration mode. Software compiled in Labview is used to control the data acquisition and processing. A typical time period used to record a frame of 2DES is about 12 min.

The instrument were covered by an aluminum box and fixed on a research grade floating optical bench (RS4000 series, Newport corporation). The whole instrument is located at the basement.

## III. RESULTS AND DISCUSSION

### A. Phase stability

The phase stability is a critical parameter for 2DES, for it is directly associated to the accuracy of the excitation frequency converted from Fourier transformation. The phase stability is more important in 2D visible spectra than that in 2D IR spectra, since the wavelength of the visible light is about one tenth of that in the IR region. Generally, the phase jitter basically arises from a number of factors such as torsional fluctuations of the mirror position and air flow which leads to a change in the refraction index of the air. A detailed protocol for characterization of phase stability of a 2D spectrometer has been proposed, which is summarized as follows [9]:

The spectrometer measures the spectrum of the sum of the two incoming interfering electric fields, *i.e.*,

$$E(t) = PE(t) + LO(t + \Delta T + \tau - \delta t) \tag{3}$$

where $PE(t)$ is the induced polarization irradiated from the medium, $LO(t+\Delta T+\tau-\delta t)$ indicates the electric filed of the local oscillator, $\Delta T$ represents the time delay between the third beam and the local oscillator, $\delta t$ is the timing jitter leading to the phase fluctuation between the two electric fields. Thus the collected spectral density:

$$S(\omega) = \tilde{E}(\omega)\tilde{E}^*(\omega) \tag{4}$$

$$S(\omega) = PE(\omega)^2 + LO(\omega)^2 + PE(\omega)LO^*(\omega) \cdot \exp[-i\omega(\Delta T + \tau) + i\delta\phi] + c.c. \tag{5}$$

$$S(\omega) = S_{PE}(\omega) + S_{LO}(\omega) + \tilde{A}(\omega)\exp[-i\omega(\Delta T + \tau)] + \tilde{A}^*(\omega)\exp[i\omega(\Delta T + \tau)] \tag{6}$$

where the phase shift is given by $\delta\phi$=$\omega\delta t$, and

$$\tilde{A}(\omega) = PE(\omega)LO^*(\omega)\exp(i\delta\phi) \tag{7}$$

DOI:10.1063/1674-0068/28/cjcp1506136 

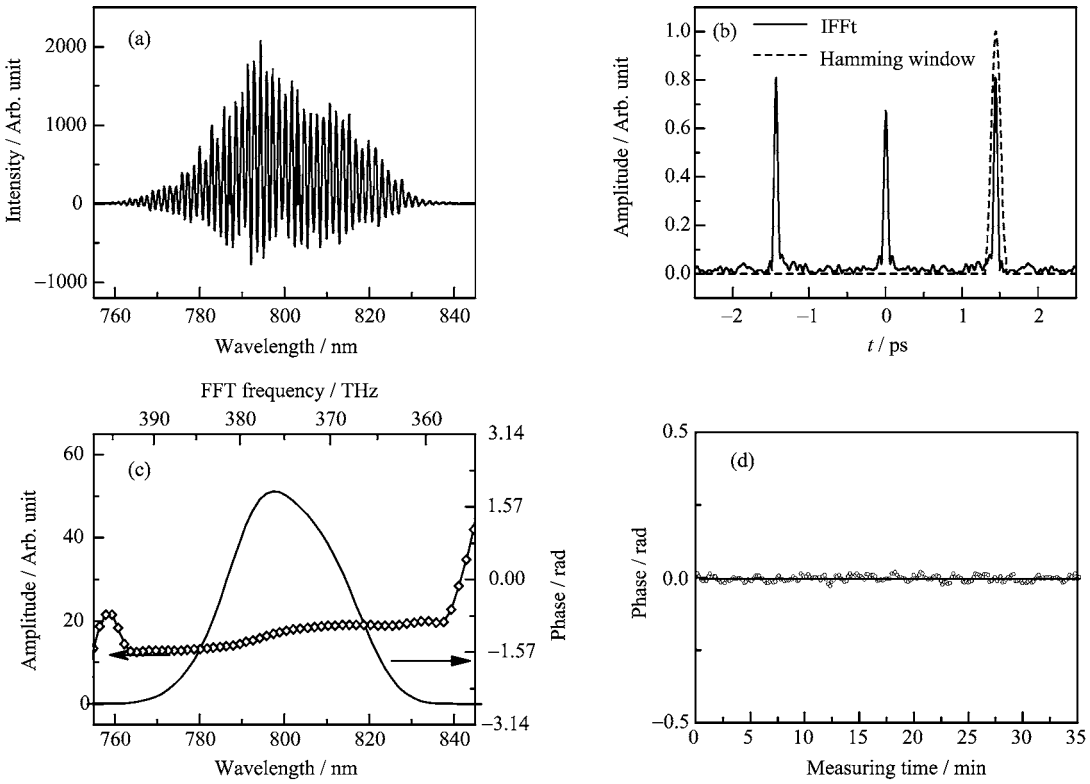


FIG. 2 Phase stability of the coherence beams 1, 2. (a) A interference spectrum of the 1, 2 beams in a random selected time delay. (b) The time signal of the interference spectrum. (c) The spectrum intensity and the phase of the spectra. (d) Phase stability between pulse 1 and pulse 2 in wavelength of 790 nm.

At first, the inverse Fourier transformation $\tilde{S}(t)$ of the interference spectrum $S(\omega)$ is performed, which gives in time domain:

$$\tilde{S}(t) = \tilde{S}_{PE}(t) + \tilde{S}_{LO}(t) + \tilde{A}(t + \Delta T + \tau) + \tilde{A}^*(t - \Delta T - \tau) \quad (8)$$

By multiplying a Hamming window ($s(t)$=0.54+ $0.46\cos(\pi t/t_{\max})$) function, $t_{\max}$ indicates the half time width of the window function, the positive part in Eq.(8) is selected.

By performing the Fourier transformation back to the frequency domain, the positive complex-conjugate spectrum can be obtained

$$\tilde{S}_+(\omega) = \tilde{A}(\omega)\exp[i\omega(\Delta T + \tau)] \quad (9)$$

After removing the oscillatory part by multiplying a factor of $\exp[-i\omega(\Delta T+\tau)]$, $\tilde{A}(\omega)$ is obtained from which the actual phase can be recovered by taking the phase:

$$\phi_s = \mathrm{Im}\{\ln[\tilde{A}(\omega)]\} \equiv \phi_0 + \delta\phi \quad (10)$$

In our experiment, we characterized the phase stability of the 2DES setup for two different cases by use of the above protocol. One is to characterize the phase stability between pulse 1 and 2, and the other is the phase stability of the photon echo signal at a fixed population and coherence time.

For the first case, pulse 3 and LO pulse were blocked and pulse 1 and 2 were focused onto another identical grating by SM3 to interfere with each other. The measured jitter of the phase difference between pulse 1 and 2 reflects the phase stability of the pulse pair after grating splitter. During the measurement, an attenuation glass with a 1 mm thickness was inserted into beam 1 to provide a fixed time delay $\Delta T'$ between pulse 1 and 2, meanwhile the intensity of pulse 1 was attenuated by a factor of 1/10 to improve the modulation contrast of the interference fringes. A typical interferogram is shown in Fig.2(a). Figure 2(b) shows the result of the inverse Fourier transformation of the given interferogram. $\tilde{A}^*(t-\Delta T')$ was selected by using a Hamming window to perform Fourier transformation. The recovered spectrum $|E(\omega)|$ together with the corresponding phase distribution are shown in Fig.2(c). Plot of the phases at 790 nm derived from 215 interferograms against the acquisition time is shown in Fig.2(d), and the standard deviation was calculated as 0.029 rad, corresponding to a phase fluctuation of $\lambda/200$, *i.e.*, the phase stability between pulse 1 and pulse 2 is about $\lambda/200$.

It has been reported that such a phase stability could be better than $\lambda/300$ [18]. However, the vibration from the environment and the air flow disturbance would de-

DOI:10.1063/1674-0068/28/cjcp1506136 

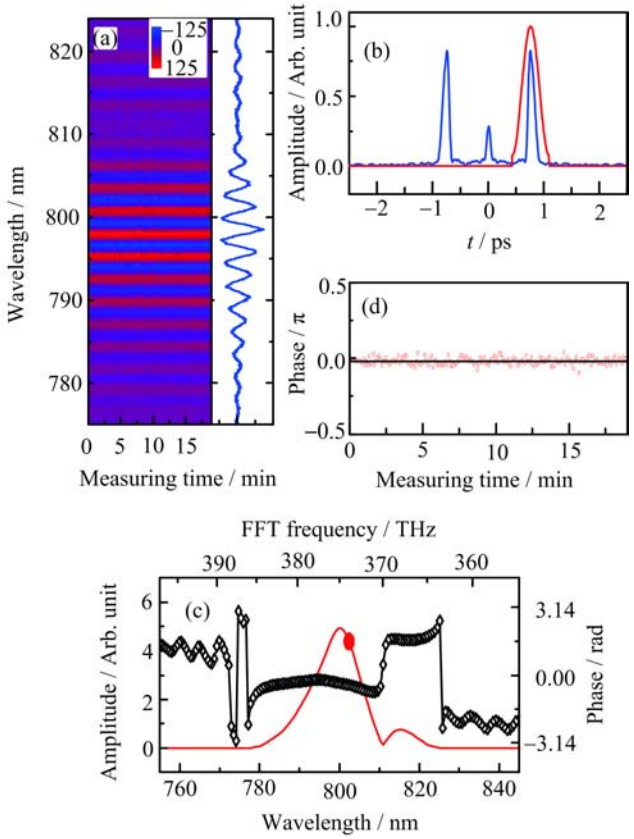


FIG. 3 (a) 200 frames of heterodyne photon echo signal recorded in 19 min ($T$=0, $\tau$=0) and spectrum in a certain time (the right panel). (b) The interference in the time domain. (c) The recovered amplitude and the phase of the signal. (d) The phase stability of the photon echo signal in 800 nm wavelength.

grade this parameter greatly.

For the second case, we measured the phase stability of the whole setup with the photon echo signal of IR140 in methanol solution by setting the population time $T$=0 and the coherence time $\tau$=0. Totally 200 interferograms were recorded in 19 min as shown in Fig.3(a), and a typical interferogram at a certain acquisition time is shown on the right panel of Fig.3(a). The corresponding result of inverse Fourier transformation, together with the Hamming window are shown in Fig.3(b), where $\tilde{A}(t+\Delta T+\tau)$, $\tilde{A}^*(t-\Delta T-\tau)$ and $\tilde{S}(t)$ are well separated since $\Delta T \gg \Delta\tau_{\rm PE}$ (the pulse width of the photon echo signal). We further perform Fourier transformation on $\tilde{A}^*(t-\Delta T-\tau)$ and remove the oscillatory part by simply shifting $\tilde{A}^*(t-\Delta T-\tau)$ to $\tilde{A}^*(t)$. The result is shown in Fig.3(c), where the spectrum (amplitude) and phase distribution are presented. Figure 3(d) plots the phase at 800 nm (with a fixed phase offset $\phi_0$) against the interferogram acquisition time, which gives a standard deviation of 0.07 rad. The result shows that a phase stability about $\lambda/90$ is achieved.

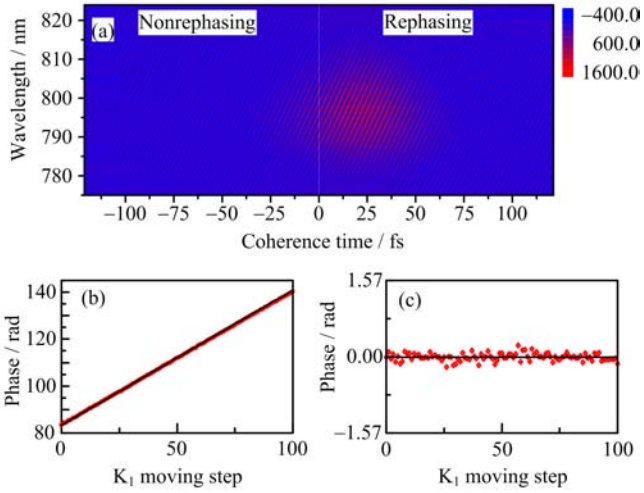


FIG. 4 (a) Raw data of IR144 resolved in methoal for $T$=0. The center wavelength is 800 nm and selected to test the frequency accuracy. (b) The phase evolution in 800 nm (black dotted line) and the linear fit (red dotted line). (c) The residual of the fitting.

### B. Frequency accuracy of instruments

For a 2D spectrum, the excitation wavelength is not measured physically, it is recovered from the coherence time $\tau$ via Fourier transformation. Acoustic perturbation and the deviations from equidistant time grid due to the positioning imperfection lead to the phase noise, which emerges as side peaks around the main peak. Acoustic perturbation can be averaged out by measuring enough long time, but the positioning imperfection is a systematic error, and it could not be averaged out, which would lead to a much worse influence [23].

It is very critical that the optical delay lines keep linear motion to guarantee an accurately Fourier transformation converted frequency. In the 2DES experiment, the translation stage ST1 or ST2 is moved to change the coherence time $\tau$ to get the rephasing or nonrephasing photon echo signals. In the current setup, the photon echo signals was measured within a coherence time window from −120 fs to 120 fs with a time step of 0.24 fs. Raw data of IR144 methanol solution at $T$=0 are presented in Fig.4(a), where the interferograms between photon echo and the LO for both rephasing and nonrephasing conditions are given at the right and left half part respectively. When ST1 is scanned from −120 fs to 0 fs, the nonrephasing signals are collected, whereas when ST2 is scanned from 0 to 120 fs, the rephasing signals are acquired accordingly.

The phase at a particular coherence time can be measured with the same method as that for the phase stability. At a given wavelength, the perfect relation between phase and the coherence time would be $\phi_0+\omega\tau$. However any deviation from the linear motion of the delay line would introduce a certain error in the determination of the frequency. As shown in Fig.4(b), the linear

DOI:10.1063/1674-0068/28/cjcp1506136 

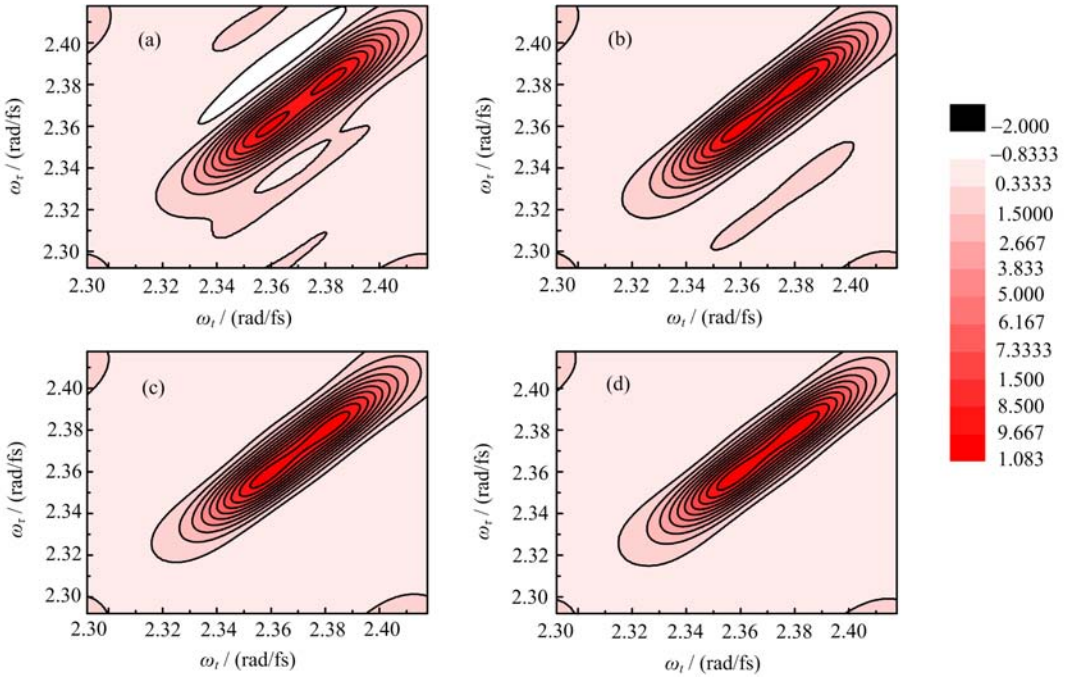


FIG. 5 Simulation of the effect of the phase jitter on the quality of the 2D spectra. Calculated 2D spectra with an introduced amount of phase jitter of (a) $\lambda/40$, (b) $\lambda/60$, (c) $\lambda/80$, and (d) 0 as the standard 2D spectra. Population time are fixed at $T$=0 fs, with $\tau_c$=0.5 ps, $\Delta$=15 rad/ps, where $\Delta$ represents frequency distribution width.

fit of the measured phase shift at 800 nm against the moving step gives a slope of 0.57 rad/step with a linear correlation coefficient of 0.99998, and the corresponding residual distribution is shown in Fig.4(c). The standard deviation of the phase fluctuations introduced by moving stage ST1 or ST2 is thus determined as $\lambda/90$.

To illustrate the effects of the phase fluctuation caused by the non-equidistant scan of the translation stage for the coherence time $\tau$, a simulation has been made. We first constructed 2D spectra of a two-level system $|1\rangle$, $|1'\rangle$ with their corresponding peak frequencies at 2.386 rad/fs (790 nm) and 2.355 rad/fs (800 nm) respectively. Their energy levels are coupled to the environment with a random fluctuation in the the corresponding frequencies, and the spectra can be described by using linear response theory expressed in terms of cumulant expansion [24]:

$$\begin{aligned} S_{1,1'}(t) = {} & \exp[-i\omega t_{1,1'}(-\tau+t)]\exp[-g(\tau)+ \\ & g(T)-g(t)-g(\tau+t)-g(T+t)+ \\ & g(\tau+t+T)]+\exp[-i\omega_{1,1'}(\tau+t)]\cdot \\ & \exp[-g(\tau)-g(T)-g(t)+g(\tau+t)+ \\ & g(T+t)-g(\tau+t+T)] \end{aligned} \tag{11}$$

where $S_{1,1'}(t)$ is the linear response function and

$$g(t)=\Delta^2\tau_c^2\left[\exp\left(-\frac{t}{\tau_c}\right)+\frac{t}{\tau_c}-1\right] \tag{12}$$

$g(t)$ is the Kubo line shape fuction, $\Delta$ represents frequency distribution width and $\tau_c$ represents correlation time. We then conducted a simple simulation of phase jitter effect on the 2D spectra of these two isolated states by addition of a certain amount of random phase jitter into the coherence time $\tau$ to simulate the nonuniform interval caused by the translation stage.

The simulation results are shown in Fig.5, which shows that the quality of the 2D spectra decreases as the amount of the introduced phase jitter increases. When the phase jitter is larger than $\lambda/60$ such as $\lambda/40$, the signal to noise ratio is pretty worse and multi-peak feature appears in the 2D spectra (Fig.5). This indicates that quality of the data with a phase jitter larger than $\lambda/60$ would be not good enough to produce reliable 2D spectra. Therefore we concluded that in the experiment the phase stability should be controlled at least better than $\lambda/60$ to guarantee the quality and the reliability of the converted 2D spectra.

### C. Phase adjustment

The final step in the data processing is the determination of the absolute phase of the 2D spectra, since the offset of the zero time between pulse 1 and pulse 2 will result in a phase shift. Also the emitted 3rd order signal and the local oscillator for heterodyne detection produce another phase error. Instead of using four laser pulses to get the $P^{(3)}$, frequency-resolved broad pump-probe experiment requires only two laser pulses for pump and probe. The first two interactions with

DOI:10.1063/1674-0068/28/cjcp1506136 

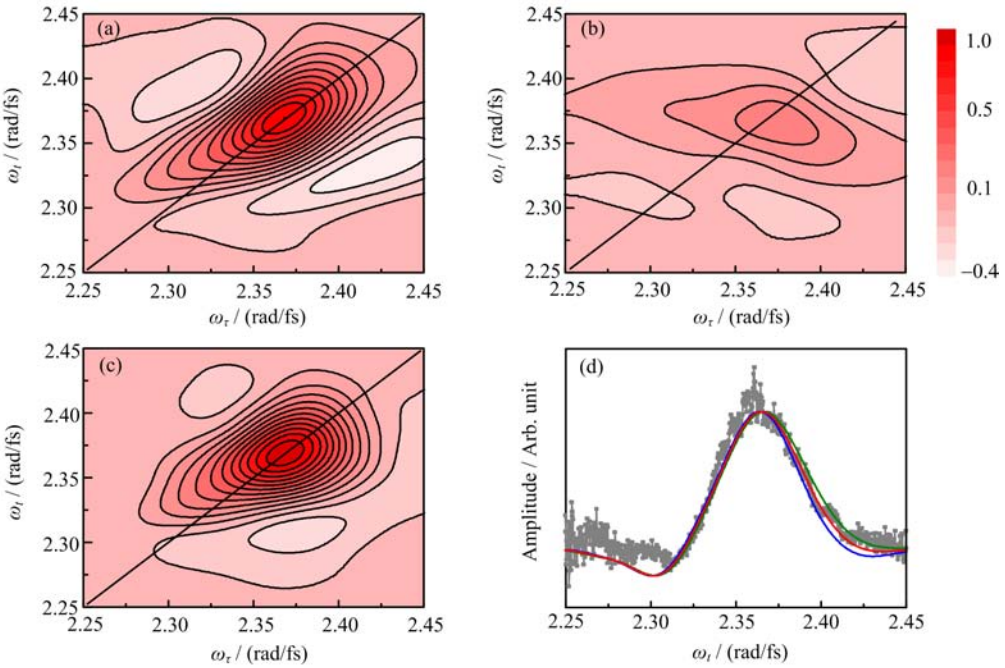


FIG. 6 Comparison of experimental 2D spectra of IR144 resolved in methanol for $T$=0 to pump probe data. (a) Rephasing signal. (b) Non-rephasing signal. (c) Absorptive signal. (d) Projection of rephasing (green), non-rephasing (blue), absorptive signal (red), and pump-probe signal (black).

the sample come from the same laser pulse so there is no timing error. And the generated third-order signal in pump-probe experiment use the second laser pulse as the local oscillator. Thus there is no timing error between the generated signal and the local oscillator. In other words, the pump-probe signal does not have the phase distortion caused by the timing errors [25].

Currently, the most commonly used criterion for phasing 2DES is the pump-probe projection.

$$A_{\mathrm{re/non}}(T,\omega_t) = \mathrm{Re}\Bigg\{\frac{\omega_t}{n(\omega_t)}\int_{-\infty}^{\infty} S_{\mathrm{re/non}}(\omega_\tau,T,\omega_t)\cdot \exp[i\Phi_c + i(\omega_t-\omega_0)t_c + i(\omega_\tau-\omega_0)\Delta\tau_{1,2}]\mathrm{d}\omega_\tau\Bigg\} \quad (13)$$

where $\omega_t$ is the spectrally resolved probe frequency, $\omega_\tau$ is the pump frequency and $\omega_0$ is the central frequency of $\omega_t$. $\Phi_c$, $\Delta\tau_{1,2}$ and $t_c$ are the added phase constant and the time shifts to adjusting the phase of the spectra. Different parameters are adjusted respectively for different population time $T$.

The pump-probe electrical field spectrum $A_{\mathrm{pp}}(T,\omega_t)$ at a delay time $T$ can be experimentally obtained by

$$A_{\mathrm{pp}}(T,\omega_t) = \frac{[I_{\mathrm{pu}}^{\mathrm{pr}}(\omega_t) - I_0^{\mathrm{pr}}(\omega_t)] - [I_{\mathrm{pu}}^{0}(\omega_t) - I_{\mathrm{b}}]}{\sqrt{I_0^{\mathrm{pr}}(\omega_t)}} \quad (14)$$

where $I_{\mathrm{pu}}^{\mathrm{pr}}(\omega_t)$ and $I_0^{\mathrm{pr}}(\omega_t)$ are the probed spectra with and without the pump beam respectively, $I_0^{\mathrm{pr}}(\omega_t)$ and $I_{\mathrm{b}}$ represent the photoluminescence from the pump beam and the stray light from the environment respectively.

The pump-probe experiment was done with the same setup with pulse 1 and 3 being blocked. Pulse 2 and LO pulse act as the pump and probe pulse setting the intensity ratio to 250:1. The projection along $\omega_\tau$ axis of both the rephasing and nonrephasing 2D spectra were compared with the results of pump-probe data to adjust the phase, as shown in Fig.6(d). After phasing, the corresponding 2D rephrasing and non-rephasing spectra are rebuilt as shown in Fig.6 (a) and (b). Figure 6(c) plots the final 2DES which combines rephasing and non-rephasing spectra. The data quality is comparable to those reported 2DES for IR144 in methanol [21].

### D. Removal of the interference from the scattering light in the pump-probe spectrum by phase-shift method

Since there is no time delay between the generated signal and the local oscillator in pump-probe spectrum, scattering of the pump beam might become a severe interference in the collected spectrum near zero time delay, which would distort the transient absorbance spectrum. Furthermore, if the sample has a significant light scattering effect, it is impossible to get a perfect overlap between the pump-probe spectrum and the 2DES projection.

Phase-shift technique has been proposed to reduce the scattering signals in 2DES by Shim and Zanni [26], which is realized by changing the phase relationship be-

DOI:10.1063/1674-0068/28/cjcp1506136 

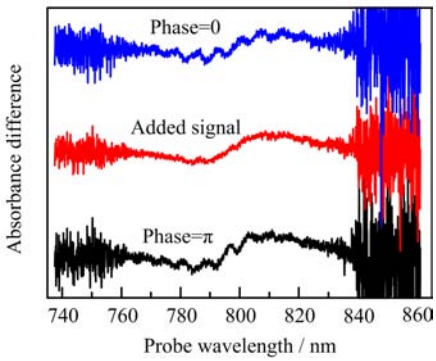


FIG. 7 Comparison of absorbance difference of B820 for population time $T$=0.14 ps with phase=0 (green) and $\pi$ (black) to the added signal (red).

tween the beams 1 and 2 or beams 3 and the local oscillator. We employ phase shift method to pump-probe experiment. By changing the pump pulse from $\phi$ to $\phi+\pi$, the phase of the scattered signal changes in accordance with the phase of pump, but that of the probe remains unchanged.

$$A_{\rm pp} \propto 2{\rm Re}(E_{\rm pump}E^*_{\rm pump}E_{\rm probe}E^*_{\rm probe} + E_{\rm scatter}E^*_{\rm probe}) \quad (15)$$

$$A^{\pi}_{\rm pp} \propto 2{\rm Re}[E_{\rm pump}\exp(i\pi)E^*_{\rm pump}\exp(-i\pi)E_{\rm probe}\cdot E^*_{\rm probe} + E_{\rm scatter}\exp(i\pi)E^*_{\rm probe}] \quad (16)$$

If we conduct pump-probe experiments with unshifted and $\pi$-phase shifted pump pulse separately and add these pump-probe signals together, the scattering terms could be canceled each other and only the pure transient absorption signals remain. To verify the proposed strategy, we performed 2DES experiment with a light harvesting complex subunit B820 as the testing sample [27, 28]. The solvent of the B820 contains high concentration of detergent which leads to a large light scattering effect possibly due to the formation of the micelles. As shown in Fig.7, there is an obvious spectral interference signal (blue and black lines) riding on the envelope of the pump-probe transient spectrum. By adding the transient spectra measured with $\pi$-phase shifted and unshifted pump pulse together, the interference has been successfully cancelled out (red line). With this transient spectrum free of scattering interference, we can adjust the phase of the projections of 2D spectra at two population time $T$=0 and $T$=80 fs respectively. It can be seen that projection of the 2D spectra matches well with the pump-probe transient spectrum. Then we rebuild the 2D spectra of B820, and the corresponding rephasing, nonrephasing and the combined absorptive 2D spectra. The results are shown in Fig.8 respectively.

Compared to the zero population, the peak shape of 2DES in 80 fs becomes more rounder, it reflects the weaker correlation between absorption frequency and emission which was caused by solvent dynamics [21]. And the spectral diffusion of each peak can be seen.

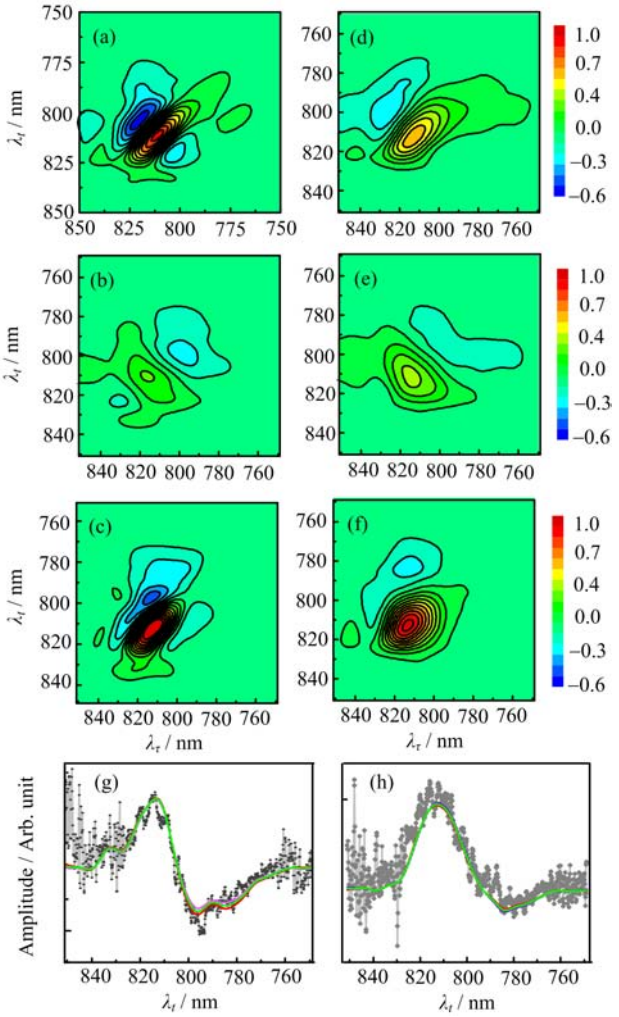


FIG. 8 2D spectra of B820 at population time equals to 0 fs ((a) rephasing, (b) nonrephasing, (c) absorptive spectra) and 80 fs ((d) rephasing, (e) nonrephasing, (f) absorptive spectra) and the projection of the 2DES at (g) 0 fs and (h) 80 fs. A clear excited absorption peak emerged in rephrasing (a, d) and absorptive (c, f) spectra.

The lower two figures show the correlation between the projection of rephasing and nonrephasing pump probe spectra. The pump-probe data were smoothed 5 points.

## IV. CONCLUSION

We have constructed a DO-based apparatus for the implementation of 2DES operating in a photon echo mode with optical heterodyne detection. The phase stability between a pulse pair split by the DO was determined to be $\lambda/200$ during an observation period of 30 min, while the phase stability of the photon echo signal is $\lambda/90$ in 19 min. The phase fluctuation introduced in the coherent time is also $\lambda/90$, which is good enough for achieving a qualified 2D spectra. The 2D spectra acquired for IR144 in methanol solution and a

DOI:10.1063/1674-0068/28/cjcp1506136 

light harvesting complex subunit B820 are comparable to those reported spectra [29].

## V. ACKNOWLEDGMENTS

The authors appreciated Dr. Lu-chao Du (Institute of physics, Chinese Academy of Sciences) for the B820 sample preparation, Prof. Jian-ping Wang (Institute of chemistry, Chinese Academy of Sciences) for help in the phase adjustment. and Prof. Yun-liang Li (Institute of physics, Chinese Academy of Sciences) for discussion about experiment. This work is supported by the National Natural Science Foundation of China (No.21227003).

[1] J. S. Waugh, Magn. Reson. Med. **7**, 253 (1988).
[2] M. L. Cowan, J. P. Ogilvie, and R. J. D. Miller, Chem. Phys. Lett. **386**, 184, (2004).
[3] S. M. G. Faeder and D. M. Jonas, J. Phys. Chem. A **103**, 10489 (1999).
[4] W. T. Pollard, S. L. Dexheimer, Q. Wang, L. A. Peteanu, C. V. Shank, and R. A. Mathies, J. Phys. Chem. **96**, 6147 (1992).
[5] T. H. Zhang, C. N. Borca, X. Q. Li, and S. T. Cundiff, Opt. Express **13**, 7432 (2005).
[6] J. D. Hybl, A. W. Albrecht, S. M. Gallagher Faeder, and D. M. Jonas, Chem. Phys. Lett. **297**, 307 (1998).
[7] J. D. Hybl, A. A. Ferro, and D. M. Jonas, J. Chem. Phys. **115**, 6606 (2001).
[8] T. Brixner, J. Stenger, H. M. Vaswani, M. Cho, R. E. Blankenship, and G. R. Fleming, Nature **434**, 625 (2005).
[9] V. I. Prokhorenko, A. Halpin, and R. J. D. Miller, Opt. Express **17**, 9764 (2009).
[10] E. Collini, C. Y. Wong, K. E. Wilk, P. M. G. Curmi, P. Brumer, and G. D. Scholes, Nature **463**, 644 (2010).
[11] P. F. Tekavec, J. A. Myers, K. L. M. Lewis, and J. P. Ogilvie, Opt. Lett. **34**, 1390, (2009).
[12] G. Panitchayangkoon, D. Hayes, K. A. Fransted, J. R. Caram, E. Harel, J. Wen, R. E. Blankenship, and G. S. Engel, Proc. Natl. Acad. Sci. USA **107**, 12766 (2010).
[13] S. T. Cundiff, A. D. Bristow, M. Siemens, H. Li, G. Moody, D. Karaiskaj, X. Dai, T. Zhang, IEEE J. Sel. Top. Quantum Electronics **18**, 318 (2012).
[14] H. Zheng, J. R. Caram, P. D. Dahlberg, B. S. Rolczynski, S. Viswanathan, D. S. Dolzhnikov, A. Khadivi, D. V. Talapin, and G. S. Engel, Appl. Opt. **53**, 1909 (2014).
[15] D. M. Jonas, Annual Rev. Phys. Chem. **54**, 425 (2003).
[16] T. Brixner, T. Mančal, I. V. Stiopkin, and G. R. Fleming, J. Chem. Phys. **121**, 4221 (2004).
[17] U. Selig, F. Langhojer, F. Dimler, T. Loehrig, C. Schwarz, B. Gieseking, and T. Brixner, Opt. Lett. **33**, 2851 (2008).
[18] G. D. Goodno, G. Dadusc, and R. J. D. Miller, J. Opt. Soc. Am. B **15**, 1791 (1998).
[19] A. A. Maznev, K. A. Nelson, and T. A. Rogers, Opt. Lett. **23**, 1319 (1998).
[20] A. A. Maznev, T. F. Crimmins, and K. A. Nelson, Opt. Lett. **23**, 1378 (1998).
[21] V. P. Singh, A. F. Fidler, B. S. Rolczynski, and G. S. Engel, J. Chem. Phys. **139**, (2013).
[22] J. F. Miller, S. B. Hinchigeri, P. S. Parkesloach, P. M. Callahan, J. R. Sprinkle, J. R. Riccobono, and P. A. Loach, Biochemistry **26**, 5055, (1987).
[23] V. Volkov, R. Schanz, and P. Hamm, Opt. Lett. **30**, 2010 (2005).
[24] Mukamel, *Principles of Nonlinear Spectroscopy*, Oxford University Press, (1995).
[25] K. Kwak, *Ph.D Dissertation*, California: Stanford University, (2008).
[26] S. H. Shim and M. T. Zanni, Phys. Chem. Chem. Phys. **11**, 748 (2009).
[27] V. Helenius, R. Monshouwer, and R. van Grondelle, J. Phys. Chem. B **101**, 10554 (1997).
[28] D. Zigmantas, Proc. Natl. Acad. Sci. USA **103**, 12672 (2006).
[29] M. Ferretti, V. I. Novoderezhkin, E. Romero, R. Augulis, A. Pandit, D. Zigmantasc, and R. van Grondelle, Phys. Chem. Chem. Phys. **16**, 9930, (2014).

DOI:10.1063/1674-0068/28/cjcp1506136 